ELSEVIER

Comput. Methods Appl. Mech. Engrg. 190 (2001) 3565–3579

Computer methods in applied mechanics and engineering

www.elsevier.com/locate/cma

Eigenfrequency optimization in optimal design

Grégoire Allaire [a,*], Sylvie Aubry [a], François Jouve [b]

[a] *Laboratoire d'Analyse Numérique, Université Paris 6, Case courrier 187, 75252 Paris Cedex 05, France*
[b] *Centre de Mathématiques Appliquées (Umr 7641), Ecole Polytechnique, 91128 Palaiseau, France*

Received 28 March 2000

Abstract

We maximize the first eigenfrequency, or a sum of the first ones, of a bounded domain occupied by two elastic materials with a volume constraint for the most rigid one. A relaxed formulation of this problem is introduced, which allows for composite materials as admissible designs. These composites are obtained by homogenization of fine mixtures of the two original materials. We prove a saddle-point theorem that permits to reduce the full (unknown) set of admissible composite designs to the smaller set of sequential laminates which is explicitly known. Although our relaxation theorem is valid only for two non-degenerate materials, we deduce from it a numerical algorithm for eigenfrequency optimization in the context of optimal shape design (i.e. when one of the two materials is void). As is the case with all homogenization methods, our algorithm can be seen as a topology optimizer. Numerical results are presented for various two- and three-dimensional problems. © 2001 Elsevier Science B.V. All rights reserved.

Keywords: Homogenization; Composite materials; Optimal design; Shape optimization; Eigenfrequency

1. Introduction

This paper is devoted to a problem of eigenfrequency maximization for a mixture of two elastic materials in a bounded domain, under a resource constraint for the most rigid material. Let Ω be a bounded open set in $\mathbb{R}^N$. Let A_1 and A_2 be two fourth-order tensors (or Hooke's laws) of two isotropic materials that are assumed to be ordered in the sense of quadratic forms, i.e., A_1 is the most compliant and A_2 the most rigid one. More precisely, we have

$$A_i = 2\mu_i I_4 + \lambda_i I_2 \otimes I_2 \quad \text{for } i = 1, 2,$$

where I_4 is the fourth-order identity, I_2 the second-order identity, and $\lambda_i = \kappa_i - 2\mu_i/N$ and κ_i, μ_i are the bulk and shear moduli, respectively, satisfying

$$0 < \kappa_1 < \kappa_2, \quad 0 < \mu_1 < \mu_2.$$

The two materials A_1 and A_2 are distributed throughout Ω. Let $\chi(x)$ denote the characteristic function of the most rigid material A_2, i.e., $\chi(x) = 1$ if A_2 is present at point x, while $\chi(x) = 0$ otherwise. The heterogeneous Hooke's law in Ω is therefore

$$A_\chi = (1 - \chi(x))A_1 + \chi(x)A_2.$$

* Corresponding author.
E-mail address: allaire@ann.jussieu.fr (G. Allaire).

0045-7825/01/$ - see front matter
PII: S0045-7825(00)00284-X

Both materials have also a positive density $\rho_1, \rho_2 > 0$ (their ordering is irrelevant). The heterogeneous density in Ω is

$$\rho_\chi = (1 - \chi(x))\rho_1 + \chi(x)\rho_2.$$

The boundary $\partial\Omega$ is divided in two disjoint parts Γ_D and Γ_N supporting respectively Dirichlet boundary condition (zero displacement) and Neumann boundary condition (zero traction). We assume that the surface measure of Γ_D is non-zero.

The vibration frequencies ω of the heterogeneous domain Ω, filled by A_1 and A_2, are the square roots of the eigenvalues of the following problem:

$$\begin{cases} -\mathrm{div} A_\chi e(u) = \omega^2 \rho_\chi u & \text{in } \Omega, \\ A_\chi e(u) \cdot \vec{n} = 0 & \text{on } \Gamma_N, \\ u = 0 & \text{on } \Gamma_D. \end{cases} \tag{1}$$

where $u(x) \in H^1(\Omega)^N$ is the displacement vector, and $e(u) = 1/2(\nabla u + \nabla^t u)$ is the strain tensor. As is well-known, problem (1) admits a countable family of positive eigenvalues

$$0 < \omega_1^2 \leqslant \omega_2^2 \leqslant \cdots \leqslant \omega_k^2 \to +\infty,$$

characterized by the min–max principle

$$\omega_k^2 = \min_{\substack{u_1,\ldots,u_k \in \mathscr{H}, \\ \dim[u_1,\ldots,u_k]=k}} \max_{u \in \mathrm{span}[u_1,\ldots,u_k]} \frac{\int_\Omega A_\chi e(u) \cdot e(u)\, \mathrm{d}x}{\int_\Omega \rho_\chi |u|^2\, \mathrm{d}x}, \tag{2}$$

where $\mathscr{H}$ is the subspace of $H^1(\Omega)^N$ made of functions satisfying $u = 0$ on Γ_D.

An important problem in structural design is to find out the best arrangement of A_1 and A_2 in Ω that would maximize the first eigenvalue, or a linear combination of the first ones. However, without further restriction on the proportion of A_1 and A_2, this problem is often trivial. For example, if $\rho_1 = \rho_2$, then the optimal solution is to fill Ω with the most rigid material A_2 only. Therefore, we add a constraint on the volume of A_2 (which may be interpreted as the additional price to pay for A_2 instead of A_1). Introducing a Lagrange multiplier $\ell \in \mathbb{R}$, our objective functional is

$$\sup_{\chi \in L^\infty(\Omega;\{0,1\})} \left\{ \omega_1^2(\chi) - \ell \int_\Omega \chi(x)\, \mathrm{d}x \right\}, \tag{3}$$

or more generally, denoting by $\alpha_k \geqslant 0$, $1 \leqslant k \leqslant p$, non-negative coefficients,

$$\sup_{\chi \in L^\infty(\Omega;\{0,1\})} \left\{ \sum_{k=1}^{p} \alpha_k \omega_k^2(\chi) - \ell \int_\Omega \chi(x)\, \mathrm{d}x \right\}. \tag{4}$$

Remark 1.1. More complicated problems fit into our framework. In particular, all our results hold if part of Ω is not subject to any optimization (such a situation is usually called a reinforcement problem). It is even possible that Ω contains a third material which is fixed and not subject to optimization. We could also consider more complex objective functionals involving non-linear expressions of the eigenfrequencies like, for example, any positive power of the eigenfrequency. Or we could mix an eigenfrequency optimization with a usual compliance optimization problem.

To simplify the exposition we focus on problem (3), but our approach works equally well for (4). For such problems we are interested in the so-called topology or layout optimization, i.e., we seek an optimal distribution of the two materials without any explicit or implicit restriction on the topology of their geometrical arrangement. Topology optimization is a major issue in structural design since classical methods of shape optimization, based on interface motion, are ill equipped to capture the possible topological complexity of the optimal mixture. This is due to the required smoothness assumptions on the interface between

the two materials that do not permit very fine mixtures, although it is widely acknowledged that they may drastically improve the performance of a candidate optimal distribution.

This practical difficulty of topology optimization has its theoretical counterpart in the fact that problems (3) and (4) are known to be generically ill-posed, i.e., they usually admit no optimal solutions (cf. the seminal counter-examples in [29,31]). Rather, one needs to enlarge the class of admissible designs by allowing for fine mixtures of the two materials on a scale which is much smaller than the mesh used for the actual computation. It is precisely the concern of the theory of homogenization to determine the effective properties of these microstructures and to select the optimal ones. Unfortunately, the set of effective Hooke's laws resulting from the mixture in fixed volume fraction of two elastic materials is unknown. This obstacle is alleviated in the particular cases where the objective functional is the elastic compliance or is an eigenfrequency because its extrema can be computed among the well-known subset of sequential laminates instead of the full set of effective tensors. This process of enlarging the space of admissible designs in order to get a well posed problem is called relaxation. The intimate connection between relaxation and homogenization is demonstrated in [31] for a scalar setting, and in [16,20–22] for elasticity.

The homogenization method for structural optimization has proved to be crucial not only for proving existence theorems of relaxed optimal designs but also for establishing necessary conditions of optimality. Since the work of Bendsoe and Kikuchi [8], a new class of numerical algorithms based on the homogenization method has appeared. They are frequently viewed as "topology optimization" algorithms since they are able to capture very fine patterns of the optimal structure on a fixed numerical grid. A few references of numerical applications of such a method include, among others, [1,2,4,6,9,10,18,35–37].

The purpose of the present paper is to extend the homogenization method, originally developed for compliance optimization, to frequency optimization problems. In the next section, a relaxed or homogenized formulation of (3) is established. Our main result is a saddle point theorem which allows to rigorously prove that the so-called sequential laminates are optimal microstructures for this problem (as they were for compliance problems, see Theorem 2.3). The spirit of this saddle point theorem is very similar to results of Lipton [25] and Cox and Lipton [11], although technically different. This theorem gives a firm theoretical basis for a numerical algorithm based on alternate directions optimization (similar to that proposed in [2] for compliance problems). In Section 3, numerical experiments demonstrate the efficiency of such an algorithm, and several technical issues are discussed at length. The homogenization method has already been applied to frequency optimization problems by several authors [7,13,14,24,28,32] (see also [6, Chapter 8]). We see at least two main differences between their works and ours: first, we prove that optimal microstructures may be chosen in the class of sequential laminates; second, we discuss a phenomenon of "spectral pollution" which arises when one of the two phases is almost degenerate.

Remark 1.2. In truth, we are interested in shape optimization, namely in the case when the most compliant material A_1 is void (all its material parameters are zero). Unfortunately, our theoretical results do not hold true in the limit when A_1 goes to zero. So we content ourselves of stating them in the case of two non-degenerate materials. From a practical point of view, this is not a too serious drawback since any numerical procedure used in topology optimization replaces void or holes by a very compliant material. Therefore, our approach agrees with the numerical common practice although it is clearly not completely satisfactory in view of the "spectral pollution" phenomenon discussed in Section 3.

2. The relaxed or homogenized formulation

This section is concerned with the relaxed formulation which is obtained from the original problem (3) by enlarging the space of admissible designs. The new generalized designs are actually composite materials obtained by homogenization of very fine microstructures of the two original materials A_1 and A_2. The importance of this relaxed or homogenized formulation is twofold. First, it makes the problem well-posed, i.e., there exist optimal generalized designs (see Proposition 2.1). Second, thanks to a saddle point theorem (see Theorem 2.3), it yields a new numerical algorithm for frequency optimization.

The derivation of the relaxed formulation is by now a standard process since the pioneering work of Murat and Tartar [31] (see also [2,4,16,20–22,26,27]). Thus, we briefly sketch it for the reader's convenience.

The starting point is to try to apply the direct method of the calculus of variations. In other words, let $\chi_n \in L^\infty(\Omega;\{0,1\})$ be a maximizing sequence for (3). We want to pass to the limit in the objective functional and compute its maximal value. Let us explain how this is possible thanks to the homogenization theory.

The sequence $\chi_n(x)$ is bounded in $L^\infty(\Omega)$, and therefore one can extract a subsequence, still denoted by $\chi_n(x)$, such that it converges weakly-* in $L^\infty(\Omega)$ to a limit $\theta(x)$. As is well-known, the limit $\theta(x)$ has no reason to be a characteristic function, but is rather a density, i.e., it belongs to $L^\infty(\Omega;[0,1])$. According to the theory of H- or G-convergence (see e.g., [15,17,30]), a subsequence of $A_{\chi_n} = (1-\chi_n(x))A_1 + \chi_n(x)A_2$ H- or G-converges to a homogenized tensor A^* as n goes to infinity. As a consequence (see e.g., [33]), the eigenvalues $0 < (\omega_1^n)^2 \leqslant (\omega_2^n)^2 \leqslant \cdots \leqslant (\omega_k^n)^2$ and the corresponding normalized eigenvectors $(u_k^n)_{k\geqslant 1}$, with $\|u_k^n\|_{L^2(\Omega)^N} = 1$, solutions of

$$\begin{cases} -\mathrm{div}\, A_{\chi_n} e(u_k^n) = (\omega_k^n)^2 \rho_{\chi_n} u_k^n & \text{in } \Omega, \\ A_{\chi_n} e(u_k^n)\cdot \vec{n} = 0 & \text{on } \Gamma_{\mathrm{N}}, \\ u_k^n = 0 & \text{on } \Gamma_{\mathrm{D}}, \end{cases} \tag{5}$$

satisfy

$$\lim_{n\to+\infty} \omega_k^n = \omega_k, \tag{6}$$

and the sequence of eigenvectors u_k^n converges, as n goes to infinity (up to a subsequence), weakly in $H^1(\Omega)^N$ and strongly in $L^2(\Omega)^N$ to a limit eigenvector u_k such that

$$\begin{cases} -\mathrm{div}\, A^* e(u_k) = (\omega_k)^2 \overline{\rho} u_k & \text{in } \Omega, \\ A^* e(u_k)\cdot \vec{n} = 0 & \text{on } \Gamma_{\mathrm{N}}, \\ u_k = 0 & \text{on } \Gamma_{\mathrm{D}}, \end{cases} \tag{7}$$

with $\overline{\rho}(x)$, the weak limit of the sequence ρ_{χ_n}, i.e.,

$$\overline{\rho}(x) = (1-\theta(x))\rho_1 + \theta(x)\rho_2.$$

Furthermore, all the eigenvalues of (7) are precisely given by the limits $0 < (\omega_1)^2 \leqslant (\omega_2)^2 \leqslant \cdots \leqslant (\omega_k)^2 \to +\infty$. Of course there is a relationship between the limit density θ and the homogenized Hooke's law A^*. Actually A^* belongs to $\mathscr{G}_\theta$, which is the subset of $L^\infty\big(\Omega;\mathscr{L}_s(\mathbb{R}_s^{N^2})\big)$ defined as

$$\mathscr{G}_\theta = \big\{H\text{-limits of } A_{\chi_n} = (1-\chi_n)A_1 + \chi_n A_2 \mid \chi_n \rightharpoonup \theta\big\}.$$

According to [12], for all $0\leqslant\theta\leqslant 1$, there exists a fixed subset G_θ of $\mathscr{L}_s(\mathbb{R}_s^{N^2})$ (the set of elasticity fourth-order tensor) such that

$$\mathscr{G}_\theta = \{A(x) \text{ measurable} \mid A(x)\in G_{\theta(x)} \text{ a.e. in } \Omega\}. \tag{8}$$

Furthermore, G_θ is the closure (in $\mathscr{L}_s(\mathbb{R}_s^{N^2})$) of the set of effective Hooke's law obtained by periodic homogenization of a mixture of A_1 and A_2 in proportions $1-\theta$ and θ. Convergence (6) allows to pass to the limit in the objective functional (3)

$$\lim_{n\to+\infty}\left\{(\omega_1^n)^2 - \ell\int_\Omega \chi_n(x)\,\mathrm{d}x\right\} = \left\{(\omega_1)^2 - \ell\int_\Omega \theta(x)\,\mathrm{d}x\right\}. \tag{9}$$

Thus, we define a relaxed functional by

$$\max_{\theta\in L^\infty(\Omega;[0,1])}\ \max_{A^*\in\mathscr{G}_\theta}\left\{\omega_1^2(\theta,A^*) - \ell\int_\Omega \theta(x)\,\mathrm{d}x\right\}, \tag{10}$$

where $\omega_1^2(\theta, A^*)$ is the first eigenvalue of (7). Since, by definition, any couple $(\theta, A^*) \in L^\infty(\Omega; [0,1]) \times \mathscr{G}_\theta$ is attained as a H- or G-limit, and because χ_n was a maximizing sequence for (3), the relaxed formulation (10) satisfies the following.

Proposition 2.1. *The homogenized formulation* (10) *is a true relaxation of the original problem* (3) *in the sense that*

1. *there exists at least one maximizer* (θ, A^*) *of* (10),
2. *any maximizing sequence* χ_n *of* (3) *converges, in the sense of homogenization, to a maximizer* (θ, A^*) *of* (10),
3. *any maximizer* (θ, A^*) *of* (10) *is attained by a maximizing sequence* χ_n *of* (3).

The outcome of Proposition 2.1 is that enlarging the space of admissible designs by allowing for composite materials (made of the two phases A_1 and A_2) makes the problem well-posed without changing its physical signification (a composite is just a fine mixture of A_1 and A_2). This has the effect of dividing the optimization process on two different lengthscales: locally at each point the microstructure has to be optimized, while globally in the domain the density distribution is also optimized.

So far, the relaxed formulation (10) is not very useful if we do not specify the set G_θ of all effective Hooke's law obtained by homogenization of A_1 and A_2 in proportion $(1-\theta)$ and θ. Unfortunately, an explicit characterization of G_θ is still pending ! Therefore, the relaxed formulation for a general objective functional is useless because of the precise class of generalized admissible designs is unknown. For compliance optimization problems the miracle is that the set G_θ can be restricted to the set L_θ of sequentially laminated composites which is better understood. In this case, the relaxed formulation is explicit and becomes amenable to numerical computations (see [2,4]). We recall the definition of the so-called finite-rank sequential laminates obtained by laminating A_2 around a core of A_1. It is based on the lamination formula of [15].

Definition 2.2. The subset $L_\theta \subset G_\theta$ of the sequential laminates obtained by laminating A_2 around a core of A_1 in proportion θ and $(1-\theta)$ respectively, is made of all Hooke's law A^*, defined by

$$(1-\theta)(A_2 - A^*)^{-1} = (A_2 - A_1)^{-1} - \theta \sum_{i=1}^{p} m_i f(e_i), \tag{11}$$

where the integer $p \geqslant 1$ is the rank of the laminate, the unit vectors $(e_i)_{1 \leqslant i \leqslant p}$ are the lamination directions, and the real numbers $(m_i)_{1 \leqslant i \leqslant p}$, satisfying $0 \leqslant m_i \leqslant 1$ and $\sum_{i=1}^{p} m_i = 1$, are the lamination parameters, and where $f(e_i)$ is a positive non-definite fourth-order tensor defined by the quadratic form (ξ being a symmetric matrix)

$$f(e)\xi \cdot \xi = \frac{1}{\mu_2}\left(|\xi e|^2 - (\xi e \cdot e)^2\right) + \frac{1}{2\mu_2 + \lambda_2}(\xi e \cdot e)^2. \tag{12}$$

It turns out that the same miracle of replacing G_θ by L_θ happens also for eigenfrequency optimization, thanks to the variational characterization (2) of the eigenvalues and to the saddle-point Theorem 2.3 below. Recall that the first eigenvalue of (7) is defined by

$$\min_{u \in \mathscr{H}} \frac{\int_\Omega A^* e(u) \cdot e(u)\, \mathrm{d}x}{\int_\Omega \overline{\rho} |u|^2\, \mathrm{d}x},$$

where $\mathscr{H}$ is the subspace of $H^1(\Omega)^N$ made of functions satisfying $u = 0$ on Γ_D. As is well-known, in full generality it is not possible to interchange a minimization and a maximization. The purpose of the next result is to prove that, in the relaxed formulation (10), it is perfectly legitimate to interchange the minimization with respect to u and the maximization with respect to A^*. As an important consequence of this saddle-point theorem, the full set G_θ of admissible designs can again be restricted to the set L_θ of sequential laminates.

Theorem 2.3. *The relaxed formulation* (10) *is equivalently given by*

$$\max_{\theta\in L^\infty(\Omega;[0,1])}\ \max_{A^*\in\mathscr{G}_\theta}\left\{\min_{u\in\mathscr{H}}\frac{\int_\Omega A^*e(u)\cdot e(u)\,\mathrm{d}x}{\int_\Omega\overline{\rho}|u|^2\,\mathrm{d}x}-\ell\int_\Omega\theta(x)\,\mathrm{d}x\right\}$$
$$=\max_{\theta\in L^\infty(\Omega;[0,1])}\left\{\min_{u\in\mathscr{H}}\frac{\int_\Omega\left(\max_{A^*\in G_\theta}A^*e(u)\cdot e(u)\right)\mathrm{d}x}{\int_\Omega\overline{\rho}|u|^2\,\mathrm{d}x}-\ell\int_\Omega\theta(x)\,\mathrm{d}x\right\}. \tag{13}$$

Furthermore, in the right-hand side of (13) *the set G_θ can be replaced by its subset L_θ of sequential laminates.*

Theorem 2.3 is similar to another saddle-point theorem proved by Lipton in [25]. Remark however that Theorem 2.3 is not a completely standard result since the Rayleigh quotient which gives the first eigenvalue is not a convex function of u. In the conductivity setting, Cox and Lipton [11] proved, as in Theorem 2.3, that the full set G_θ can be restricted to the set L_θ. Let us emphasize that Proposition 2.1 and Theorem 2.3 hold true also for the objective functional (4), involving several eigenvalues.

Remark 2.4. When the objective functional involves a first eigenvalue (as is the case with (3) and (10)), which is simple, Theorem 2.3 can be slightly improved by using a further property of the optimal sequential laminate in (13). It is well known that, for a single energy, the optimal laminate is, at most, of rank N (the space dimension), and that the lamination directions are aligned with the principal strains and stresses (see e.g., [3,23]). Therefore, in the right-hand side of (13), one can further restrict L_θ to its subspace of rank-N sequential laminate with lamination directions given by the eigenvectors of the strain tensor $e(u)$ (for explicit formulae, see [2,16,18]). However, for a multiple first eigenvalue or for an objective functional involving several eigenvalues, like (4), there is no explicit formula for the optimal laminate which may be of rank higher than N.

Remark 2.5. In the relaxed formulation (10)–(13), it is not possible to exchange the maximization with respect to θ and the minimization with respect to u since, for fixed u, the right-hand side of (13) has no concavity properties. Even more, for $A^*\in L_\theta$ defined by (11), the energy $A^*e(u)\cdot e(u)$ is a convex function of θ, and thus $\max_{A^*\in G_\theta}A^*e(u)\cdot e(u)$ is also convex in θ.

The remainder of this section is devoted to the proof of Theorem 2.3. Those readers who are willing to accept it may skip the rest of this section in a first pass.

Proof of Theorem 2.3. Let $\theta(x)$ be a fixed function in $L^\infty(\Omega;[0,1])$. Recall that $\mathscr{G}_\theta$ is defined by (8). Similarly we define

$$\mathscr{L}_\theta=\{A(x)\ \text{measurable}\mid A(x)\in L_{\theta(x)}\ \text{a.e. in}\ \Omega\},$$

which satisfies $\mathscr{L}_\theta\subset\mathscr{G}_\theta$ since for any $\theta_0\in[0,1]$, $L_{\theta_0}\subset G_{\theta_0}$. Thus, we have

$$\max_{A^*\in\mathscr{G}_\theta}\min_{u\in\mathscr{H}}\frac{\int_\Omega A^*e(u)\cdot e(u)\,\mathrm{d}x}{\int_\Omega\overline{\rho}|u|^2\,\mathrm{d}x}\geqslant\sup_{A^*\in\mathscr{L}_\theta}\min_{u\in\mathscr{H}}\frac{\int_\Omega A^*e(u)\cdot e(u)\,\mathrm{d}x}{\int_\Omega\overline{\rho}|u|^2\,\mathrm{d}x}. \tag{14}$$

(For a given function θ, the existence of a maximizer $A^*\in\mathscr{G}_\theta$ for the left-hand side of (14) is guaranteed by the homogenization theory.) By a result of Avellaneda [5], for each tensor $A_0^*\in G_{\theta_0}$ there exists another tensor $B_0^*\in L_{\theta_0}$ such that $A_0^*\leqslant B_0^*$ in the sense of quadratic forms on the space of symmetric matrices. This result easily extends to a tensor-valued function $A^*\in\mathscr{G}_\theta$ for which there exists another tensor-valued function $B^*\in\mathscr{L}_\theta$ such that

$$A^*(x)\leqslant B^*(x)\ \text{a.e.}\ x\in\Omega.$$

(This is obvious for piecewise constant function A^*, and since such tensors are dense in $\mathscr{G}_\theta$ for the strong $L^p(\Omega)$ topology with $1\leqslant p<+\infty$, a density argument yields the desired result upon noticing the closed character of G_θ and L_θ.) Clearly, it implies the converse inequality of (14) and the supremum in $\mathscr{L}_\theta$ is attained, i.e.,

$$\max_{A^*\in\mathscr{G}_\theta}\min_{u\in\mathscr{H}}\frac{\int_\Omega A^*e(u)\cdot e(u)\,\mathrm{d}x}{\int_\Omega\overline{\rho}|u|^2\,\mathrm{d}x}=\max_{A^*\in\mathscr{L}_\theta}\min_{u\in\mathscr{H}}\frac{\int_\Omega A^*e(u)\cdot e(u)\,\mathrm{d}x}{\int_\Omega\overline{\rho}|u|^2\,\mathrm{d}x}. \tag{15}$$

On the other hand, another application of Avellaneda's result [5] shows that locally the set G_θ can also be replaced by the set L_θ of sequential laminates, i.e.,

$$\max_{A^*\in G_\theta}A^*e(u)\cdot e(u)=\max_{A^*\in L_\theta}A^*e(u)\cdot e(u).$$

Remarking that, in view of definition (8) of $\mathscr{G}_\theta$, the constraint $A^*\in\mathscr{G}_\theta$ is local, for a given function $u\in\mathscr{H}$ we deduce

$$\max_{A^*\in\mathscr{G}_\theta}\frac{\int_\Omega A^*e(u)\cdot e(u)\,\mathrm{d}x}{\int_\Omega\overline{\rho}|u|^2\,\mathrm{d}x}=\frac{\int_\Omega\left(\max_{A^*\in G_\theta}A^*e(u)\cdot e(u)\right)\mathrm{d}x}{\int_\Omega\overline{\rho}|u|^2\,\mathrm{d}x}=\frac{\int_\Omega\left(\max_{A^*\in L_\theta}A^*e(u)\cdot e(u)\right)\mathrm{d}x}{\int_\Omega\overline{\rho}|u|^2\,\mathrm{d}x}$$
$$=\max_{A^*\in\mathscr{L}_\theta}\frac{\int_\Omega A^*e(u)\cdot e(u)\,\mathrm{d}x}{\int_\Omega\overline{\rho}|u|^2\,\mathrm{d}x}.$$

Therefore, the min–max equality (13) is proved if we can show that

$$\max_{A^*\in\mathscr{L}_\theta}\min_{u\in\mathscr{H}}\frac{\int_\Omega A^*e(u)\cdot e(u)\,\mathrm{d}x}{\int_\Omega\overline{\rho}|u|^2\,\mathrm{d}x}=\min_{u\in\mathscr{H}}\max_{A^*\in\mathscr{L}_\theta}\frac{\int_\Omega A^*e(u)\cdot e(u)\,\mathrm{d}x}{\int_\Omega\overline{\rho}|u|^2\,\mathrm{d}x}, \tag{16}$$

where $\mathscr{H}$ is the subspace of $H^1(\Omega)^N$ made of functions vanishing on Γ_{D}.

The proof of equality (16) is based on the following remark of [5]. Denoting by S^{N-1} the unit sphere in $\mathbb{R}^N$, L_θ is equivalently defined as the set of all fourth-order tensors $A^*(v)$ given by

$$(1-\theta)(A_2-A^*(v))^{-1}=(A_2-A_1)^{-1}-\theta\int_{S^{N-1}}f(e)\,\mathrm{d}v(e), \tag{17}$$

where $v(e)$ is any probability measure on S^{N-1}, namely $v\geqslant 0$ and $\int_{S^{N-1}}\mathrm{d}v(e)=1$ (in particular, (17) implies that L_θ is closed). We denote by P the convex set of such probability measure on S^{N-1}. Before going on, we simplify a little the notations. Let us define $\mathscr{B}$ by

$$\mathscr{B}=\left\{u\in\mathscr{H}\;|\;\int_\Omega\overline{\rho}|u|^2\,\mathrm{d}x=1\right\},$$

which, by Rellich theorem, is a closed set for the weak topology in $\mathscr{H}$. Let us also define a function $g(u,v)$ from $\mathscr{B}\times L^\infty(\Omega;P)$ into $\mathbb{R}^+$ by

$$g(u,v)=\int_\Omega A^*(v)e(u)\cdot e(u)\,\mathrm{d}x,$$

where $A^*(v)$ is given by (17). With these notations (16) is equivalent to

$$\max_{v\in L^\infty(\Omega;P)}\min_{u\in\mathscr{B}}g(u,v)=\min_{u\in\mathscr{B}}\max_{v\in L^\infty(\Omega;P)}g(u,v). \tag{18}$$

As proved in [25], for a given $u\in\mathscr{H}$, the function $v\to g(u,v)$ is concave in $L^\infty(\Omega;P)$ (remark that $u\to g(u,v)$ is also convex in $H^1(\Omega)^N$ but unfortunately not in $\mathscr{B}$). Note that, for fixed v, there always exists a minimizer (possibly non-unique) $u\in\mathscr{B}$ of $g(u,v)$: it is just a first eigenvector of the Hooke's law $A^*(v)$ corresponding to the first eigenvalue $\min_{u\in\mathscr{B}}g(u,v)$ (which may have a multiplicity larger than one). The function $v\to\min_{u\in\mathscr{B}}g(u,v)$ is also concave (as the minimum of concave functions) on the convex set $L^\infty(\Omega;P)$, and it admits, at least, one maximizer v^* because the maxima in (15) are attained. Of course, for this measure v^*, there exists a non-unique minimizer u^* in $\mathscr{B}$ of $g(u,v^*)$. We shall prove that there exists a choice of minimizer $u^*\in\mathscr{B}$ of $g(u,v^*)$ such that (u^*,v^*) is a saddle point of $g(u,v)$, i.e., for any $u\in\mathscr{B}$ and any $v\in L^\infty(\Omega;P)$

$$g(u^*, v) \leqslant g(u^*, v^*) \leqslant g(u, v^*). \tag{19}$$

Then, it is a classical result in the calculus of variations to show that (19) implies the desired result (18). The second inequality of (19) is obvious since it is just the definition of u^* as a minimizer of $g(u, v^*)$. To prove the first inequality of (19), we introduce, for any measure $v \in L^\infty(\Omega; P)$ and for any $t \in [0,1]$, a measure $v(t) = tv + (1-t)v^*$ which, by convexity, also belongs to $L^\infty(\Omega; P)$. Let $u(t)$ denote a minimizer in $\mathscr{B}$ of $g(u, v(t))$. Since v^* is a maximizer of $\min_{u\in\mathscr{B}} g(u, v)$, we have

$$g(u^*, v^*) \geqslant g(u(t), v(t)), \tag{20}$$

which implies that, as t goes to 0, the sequence $u(t)$ is bounded in $H^1(\Omega)^N$. Therefore, there exists a limit $\tilde{u}$ such that, up to a subsequence $u(t)$ converges to $\tilde{u}$ weakly in $H^1(\Omega)^N$ and strongly in $L^2(\Omega)^N$ by Rellich theorem. Thus, $\tilde{u}$ belongs to $\mathscr{B}$ too. Since $v(t)$ converges strongly to v^* in $L^\infty(\Omega; P)$, as t goes to 0, the convexity of $g(u, v)$ with respect to u in $H^1(\Omega)^N$ (and not in $\mathscr{B}$) implies

$$\lim_{t\to 0} g(u(t), v(t)) \geqslant g(\tilde{u}, v^*),$$

which, in view of (20), proves that $\tilde{u}$ is also a minimizer of $g(u, v^*)$ in $\mathscr{B}$. Hence, from now on, our choice of minimizer u^* is $u^* = \tilde{u}$. By concavity of $g(u, v)$ with respect to v, we have

$$g(u(t), v(t)) \geqslant tg(u(t), v) + (1-t)g(u(t), v^*) \geqslant tg(u(t), v) + (1-t)g(u^*, v^*). \tag{21}$$

Combining (20) and (21), for $t > 0$ we deduce

$$g(u^*, v^*) \geqslant g(u(t), v).$$

Then, letting t goes to zero, by convexity of $g(u, v)$ with respect to u in $H^1(\Omega)^N$, we obtain

$$g(u^*, v^*) \geqslant g(u^*, v)$$

which completes the proof of the saddle-point result (19).

Remark 2.6. The key ingredients in the proof of the saddle-point inequality (19) are the convexity of $u \to g(u, v)$ in $H^1(\Omega)^N$ (although not in $\mathscr{B}$), and the closeness of $\mathscr{B}$ for the weak topology of $H^1(\Omega)^N$. These two arguments are still valid for more general objective functionals involving a sum of eigenvalues. Therefore, Theorem 2.3 holds true also in this latter case.

3. Numerical algorithms for frequency optimization

This section presents the proposed numerical algorithms for eigenfrequency optimization, which are based on the homogenization method. The first one is an optimality criteria method and is very similar to those introduced in [2] for compliance optimization and [7,13] for eigenfrequencies optimization. The second one is a gradient method, which is slower but more stable, at least when the first eigenvalue remains simple (and thus differentiable). In both cases the key idea is to compute "generalized" optimal designs for the relaxed formulation, rather than "classical" designs which are merely approximately optimal for the original formulation. In a final stage classical designs are recovered from generalized ones by an adequate penalization procedure which removes all the intermediate density regions from the final result.

Our first algorithm is an alternate direction optimization using optimality criteria for the relaxed formulation

$$\max_{\theta\in L^\infty(\Omega;[0,1])} \left\{ \min_{u\in\mathscr{H}} \frac{\int_\Omega \left(\max_{A^*\in G_\theta} A^* e(u)\cdot e(u)\right) \mathrm{d}x}{\int_\Omega \overline{\rho}|u|^2 \,\mathrm{d}x} - \ell \int_\Omega \theta(x)\,\mathrm{d}x \right\}. \tag{22}$$

We see (22) as a saddle point problem, and optimize separately and iteratively in θ, A^*, u. This is perfectly legitimate for A^*, u since (22) is a saddle function with respect to these two variables. However, this strategy may be discussed concerning θ since the maximization with respect to θ cannot be interchanged with the

other optimizations. Eventually, the computation of a generalized optimal design is followed by a penalization procedure which "projects" this generalized design on the space of classical designs. This procedure amounts to run a few more iterations where the density θ is forced to take values close to 0 or 1 (for details, see [2]). Consequently, the algorithm is structured as follows:

1. Initialization of the design parameters (θ_0, A_0^*) by taking $\theta_0 = 1$ and $A_0^* = A_2$ everywhere in the domain.
2. Iteration until convergence:
   (a) Computation of u_n through a problem of linear elasticity with $(\theta_{n-1}, A_{n-1}^*)$ as design variables.
   (b) Updating of the design variables (θ_n, A_n^*) for fixed u_n.

Convergence of this iterative algorithm is detected when the objective function becomes stationary, or when the change in the design variables becomes smaller than some preset threshold. The initialization can also be done with a uniform composite material of given density $\theta_0 \neq 1$, in order to initially satisfy the volume constraint.

The optimality condition for A^* is simple. Assuming that the first eigenvalue remains simple (which is the case in all computations below), it can be chosen pointwise in the computational domain as a rank-N sequential laminate which maximizes the Hashin–Shtrikman bound

$$\max_{A^* \in G_\theta} A^* e(u) \cdot e(u). \tag{23}$$

Alternatively, the bound (23) is equivalent (through a Legendre transform) to the following one

$$\min_{A^* \in G_\theta} A^{*-1} \sigma \cdot \sigma, \tag{24}$$

namely an optimal A^* in (23) is also optimal in (24) for $\sigma = A^* e(u)$. Since we have explicit formula for an optimal rank-N sequential laminate in (24) (see [2]), we rather use (24) instead of (23) for updating the tensor A^*. More precisely, in step (b) we compute A_n^* given by formula (11): its lamination directions $(e_i)_{1 \leqslant i \leqslant N}$ are the principal directions of $\sigma_n = A_{n-1}^* e(u_n)$, its lamination parameters $(m_i)_{1 \leqslant i \leqslant N}$ are optimized in terms of the eigenvalues of $\sigma_n = A_{n-1}^* e(u_n)$ (see [2] for details).

The optimality condition with respect to θ is troublesome. Indeed as remarked in [18], for fixed u, the elastic energy $\int_\Omega A^* e(u) \cdot e(u)$ is convex in θ when A^* is a sequential laminate given by (11). Similarly, the function $(\int_\Omega \overline{\rho} |u|^2)^{-1}$ is also convex in θ. We do not know if the product of the two is convex (except in the obvious cases where either the phase densities are equal or the phase elastic moduli are equal). Nevertheless, it indicates that this optimality condition will have a tendency to produce 0/1 values of θ, and will be unable to predict precise intermediate values. On the other hand, in the context of compliance optimization for one loading case, we use a stress formulation which yields an explicit optimality condition for the density θ in terms of the stress. This later condition is much more satisfying since it corresponds to minimizing a convex function of θ. For this reason, by the Legendre transform, we rewrite the elastic energy

$$A^* e(u) \cdot e(u) = \max_\sigma \left(2e(u) \cdot \sigma - A^{*-1} \sigma \cdot \sigma \right),$$

where the maximum is attained by the true stress $\sigma = A^* e(u)$. For simplicity, we do not take into account the denominator $(\int_\Omega \overline{\rho} |u|^2)^{-1}$ in the optimality conditions. With all these simplifications, we compute the density θ_n as the unique maximizer of the following function

$$f(\theta) = -\frac{\int_\Omega A_n^{*-1}(\theta) \sigma_n \cdot \sigma_n \, \mathrm{d}x}{\int_\Omega \overline{\rho}(\theta_{n-1}) |u_n|^2 \, \mathrm{d}x} - \ell \int_\Omega \theta(x) \, \mathrm{d}x.$$

In other words, θ_n is the unique minimizer of $-f(\theta)$ which is a convex function of θ (see [2]). The explicit formulae for updating the effective tensor A_n^* and the density θ_n are therefore the same as those used for compliance optimization problems (cf. Remark 2.4). These formulae, giving the optimal sequential laminate, can be found in [4] for 2-D, and in [2] for 3-D. We use an additional procedure adjusting at each iteration the value of the Lagrange multiplier ℓ to keep constant the total amount of material.

In the following numerical examples, the workspace Ω is discretized with quadrangular (resp. hexaedral) elements in 2-D (resp. 3-D). The displacement is approximated by $Q1$ interpolation and the resulting stress field is averaged on each cell. The effective Hooke's law is constant on each element.

All the computations are performed with the bulk modulus κ and the shear modulus 2μ equal to 1. The density ρ_2 is equal to 1 and the density ρ_1 of the weak material is equal to 10^{-3}. The smallest admissible value of θ and for the proportions m_i is 10^{-3}, in order to avoid very low proportions. In practice, the value of this parameter is insignificant; any small number produces similar results. The density θ is represented with a gray scale: areas where $\theta = 1$ (pure material) are black, whereas white zones correspond to voids. Gray zone represent composite material.

As a first example, we show in Fig. 1 the computed design of a 2-D cantilever. The workspace Ω is a 1×2 rectangle, with a small fixed zone of density 10 in the middle of the upper side. This part is not subject to optimization and its Lamé coefficient are the same as in the rest of the domain (Fig. 1-left). The first eigenvalue is maximized with a weight constraint of 35% of the total volume. Fig. 1 shows the composite (middle) and the penalized solution (right). The lowest eigenvalue of the composite design is multiplied by a factor 9.04 compared to the first eigenvalue of the domain filled with a uniform isotropic composite material of density 0.35 (to satisfy the volume constraint). The penalized design has his first eigenvalue multiplied by 8.10.

For this test-case, the convergence is smooth. A nice property of the algorithm for compliance optimization is the non-dependence of the solution with respect to the initial configuration. Fig. 2 shows different steps of the algorithm for this example, when initialized with a "bad" configuration (the composite solution turned upside-down). The stable solution is obtained after a few more iterations than in the previous case. Fig. 3 is a plot of the first eigenvalue as a function of the algorithm's iterations in both cases (the peaks are due to a bad adjustment of the volume constraint at the beginning of the penalization process).

As pointed out by some authors (see e.g., [7]) such kind of algorithms may show oscillations for some test-cases, leading sometimes to non-convergence of the numerical method. Indeed, there is no guaranty that this algorithm always increases the first eigenvalue. More than that, when the most compliant phase A_1 is almost degenerate, mimicking void, the first eigenvalue does not necessarily correspond to an eigenvector supported mainly in the solid phase A_2. One possible explanation is that spurious eigenvalues appear which correspond to vibrations of the weak phase only and have nothing to do with the optimized structure. This phenomenon of "spectral pollution" is due to the process of replacing void by a very compliant phase, which is clearly not correct in such a case. It has been rigorously analyzed in a similar

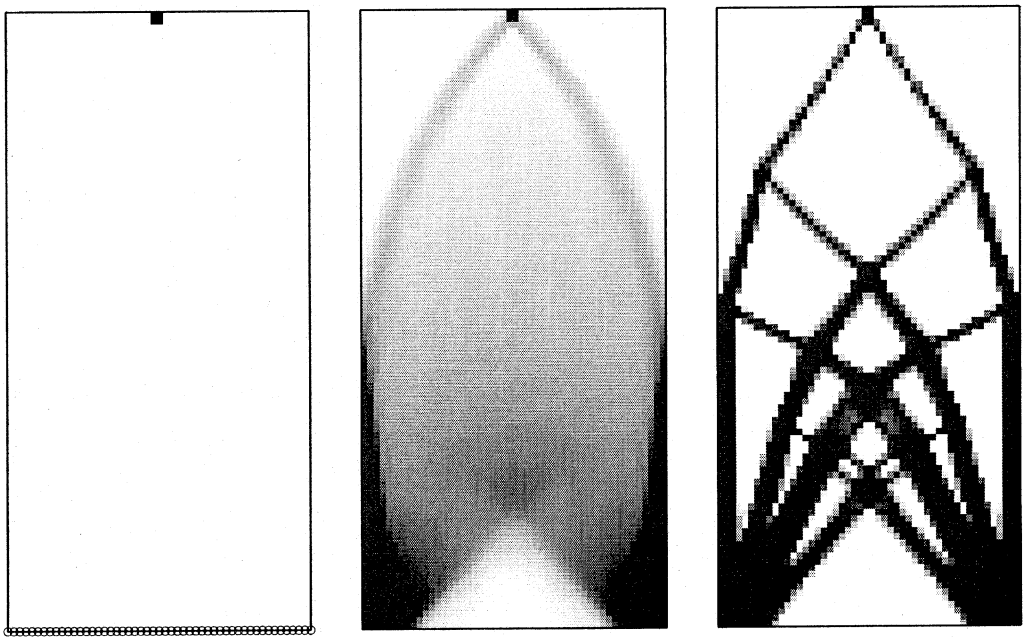

Fig. 1. Left: computation domain and boundary conditions for the "vertical" cantilever. Middle: composite solution. Right: penalized solution.

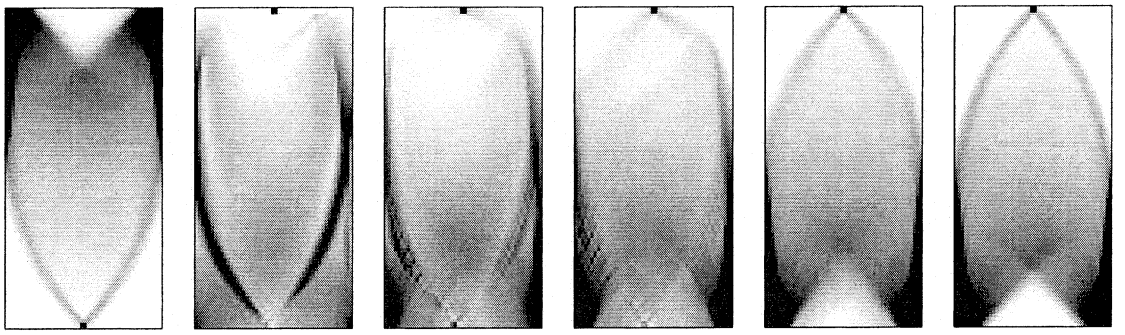

Fig. 2. Evolution of the design during the algorithm. Left to right: initial configuration and iterations 1, 4, 10, 40 and 154 (final).

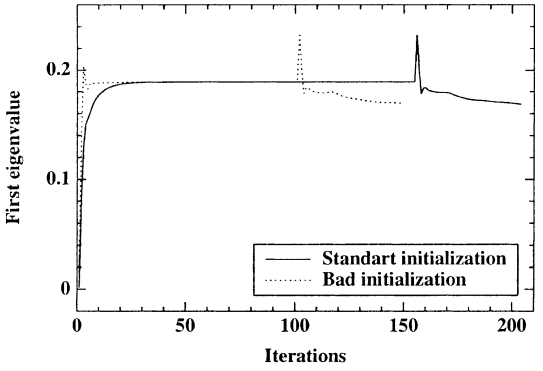

Fig. 3. History of the first eigenvalue for two different initial configurations

context in Section VII.1 of [34]. Numerically, this process starts as follows: after a number of iterations of our above optimality criteria algorithm, during which the shape evolves smoothly and the first eigenvalue increases, the shape breaks down quickly and the first eigenvalue oscillates below its previous value. This phenomenon has nothing to do with a possible crossing of different modes and the first eigenvalue remains simple. The algorithm has a tendency to produce zones which oscillate from low to high density between two successive iterations. There are well-known remedies for stabilizing these types of computations (filtering high strains in void region, following the right mode by orthogonality of successive eigenvectors), but they are purely numerical tricks with no firm rigorous background. We have to recognize that the onset of these instabilities is still mysterious for us.

Fig. 4 shows an example of blow-up of the solution in our first algorithm. The configuration of the test-case is very similar to the previous one, except that the workspace is a rectangle 2×1. The solution is drawn for different iterations.

In order to avoid this breakdown of the optimality criteria method we propose a second algorithm which is a gradient method. Of course, a gradient method for maximizing the first eigenvalue is valid as long as the first eigenvalue is simple and thus differentiable with respect to the design parameters (the same holds true for any combination of the first eigenvalues). It ensures that the first eigenfrequency will always increase through the iterations (although it can fall into a local maximum). We describe its 2-D implementation (there is no conceptual difficulty for extending it to 3-D). By a matter of theory (cf. Remark 2.4), the optimal laminate can always be chosen as a rank-2 laminate with orthogonal directions. Therefore, the design parameters are the density $\theta \in [0,1]$, the angle of rotation $\alpha \in [0,\pi]$, and the proportion $m \in [0,1]$. In other words, the homogenized Hooke's law $A^*(\theta,\alpha,m)$ is now given locally by

$$(1-\theta)(A_2 - A^*(\theta,\alpha,m))^{-1} = (A_2 - A_1)^{-1} - \theta Q(\alpha)^{-1}(mf(e_1) + (1-m)f(e_2))Q(\alpha), \tag{25}$$

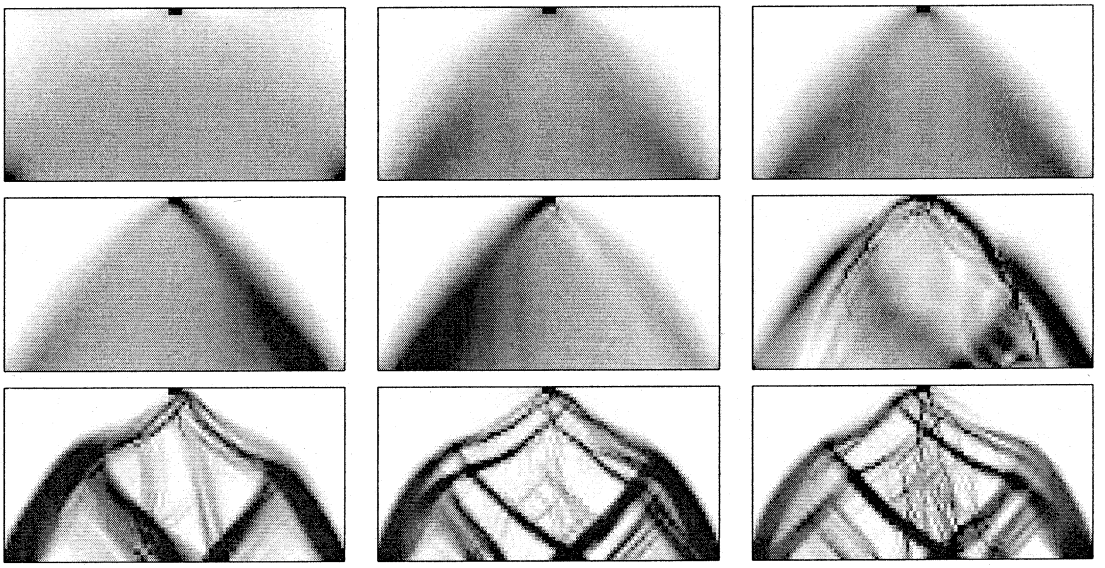

Fig. 4. Evolution of the design during the algorithm. Left to right: iteration number 1, 3, 7, 11, 12, 15, 25, 75, 100.

where (e_1, e_2) is a fixed orthonormal basis of $\mathbb{R}^2$ and $Q(\alpha)$ is the fourth-order tensor corresponding to a rotation of angle α in the physical space $\mathbb{R}^2$. The relaxed optimal design problem (10) is therefore equivalent to

$$\max_{\theta\in L^\infty(\Omega;[0,1])}\ \max_{\alpha\in L^\infty(\Omega;[0,\pi])}\ \max_{m\in L^\infty(\Omega;[0,1])}\left\{\omega_1^2(\theta,\alpha,m)-\ell\int_\Omega\theta(x)\,\mathrm{d}x\right\},$$

where ω_1^2 is the first eigenvalue of (7). As is well-known, the computation of the partial derivatives with respect to these parameters is easy when the first eigenvalue is simple and is more tricky if it is multiple. To avoid any difficulties, we assume that the parameters $(\theta,\alpha,m)\in L^\infty(\Omega;[0,1]\times[0,\pi]\times[0,1])$ are such that the first eigenvalue $\omega_1^2(\theta,\alpha,m)$ is simple. Then, for a given direction $(\delta\theta,\delta\alpha,\delta m)\in L^\infty(\Omega)^3$ we define a function of t in the neighborhood of 0 by

$$f(t)=\omega_1^2(\theta+t\delta\theta,\alpha+t\delta\alpha,m+t\delta m). \tag{26}$$

By a classical result of spectral perturbation (see e.g. [19], or Theorem 9.10 in [34]), for sufficiently small non-negative values of t the first eigenvalue in (26) is simple and $f(t)$ is differentiable. The computation of $\mathrm{d}f/\mathrm{d}t(0)$ is just a matter of algebra and the result is given in the following lemma.

Lemma 3.1. *Assume that the first eigenvalue $\omega_1^2(\theta,\alpha,m)$ is simple at $(\theta,\alpha,m)\in L^\infty(\Omega;[0,1]\times[0,\pi]\times[0,1])$. Then, it is Gateaux differentiable with partial derivatives given by*

$$\nabla_\theta(\omega_1^2)=\frac{(\nabla_\theta A^*)e(u)\cdot e(u)-\omega_1^2(\rho_2-\rho_1)|u|^2}{\int_\Omega\overline{\rho}|u|^2}-\ell,$$

$$\nabla_m(\omega_1^2)=\frac{(\nabla_m A^*)e(u)\cdot e(u)}{\int_\Omega\overline{\rho}|u|^2},$$

$$\nabla_\alpha(\omega_1^2)=\frac{(\nabla_\alpha A^*)e(u)\cdot e(u)}{\int_\Omega\overline{\rho}|u|^2},$$

where u is a first eigenvector for (7) *associated to the first eigenvalue* $\omega_1^2(\theta,\alpha,m)$ *and*

$$\nabla_\theta A^* = B^{-1}(\theta,m,\alpha) + (\theta-1)B^{-1}(\theta,m,\alpha)T(m,\alpha)B^{-1}(\theta,m,\alpha),$$
$$\nabla_m A^* = \theta(\theta-1)B^{-1}(\theta,m,\alpha)(f(e_1)-f(e_2))B^{-1}(\theta,m,\alpha),$$
$$\nabla_\alpha A^* = -\theta(\theta-1)B^{-1}(\theta,m,\alpha)(\nabla_\alpha T(m,\alpha))B^{-1}(\theta,m,\alpha),$$

with

$$T(m,\alpha) = Q^{-1}(\alpha)(mf(e_1)+(1-m)f(e_2))Q^{-1}(\alpha),$$

and

$$B(\theta,m,\alpha) = (A_2-A_1)^{-1} - \theta T(m,\alpha).$$

Of course, since there are constraints on the parameters m and θ (that must stay both between 0 and 1), the formulas of Lemma 3.1 are combined with a projection step in order to satisfy the constraints (including also the total weight constraint). A line search is performed to compute a good descent step in this projected gradient algorithm. Because of the high cost of the line search (each evaluation of the objective function is an eigenvalue problem), the gradient method is more expensive than the optimality criteria. Therefore, in practice our strategy is to start with the optimality criteria method and to switch to the gradient method only when the computed first eigenvalue becomes lower than the previous one.

Fig. 5 is a plot of the convergence history of the method for the cantilever 2×1 described before. The algorithm using explicit formulae is compared to the new algorithm using the projected gradient. The new algorithm switches to the projected gradient after seven iterations. The erratic comportment of the first algorithm is clearly visible on this plot, while the gradient method is stable and converges smoothly. Fig. 6 shows the resulting composite solution. The first eigenvalue is multiplied by a factor 5.03. We compared this solution with the "usual" cantilever solution obtained by compliance optimization (two bars meeting at right angle): the first eigenvalue for this latter shape is about 0.43, to be compared with the obtained value of 1.43 for the optimal composite shape.

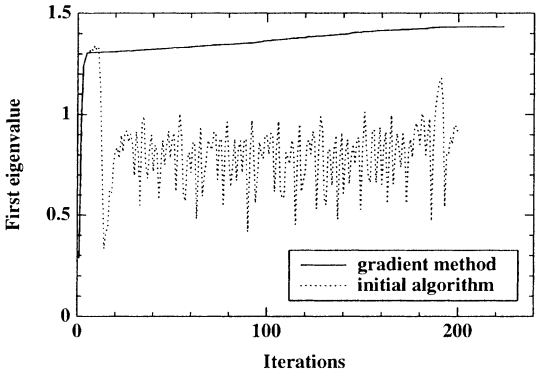

Fig. 5. Evolution of the first eigenvalue with both algorithms for the cantilever 2×1.

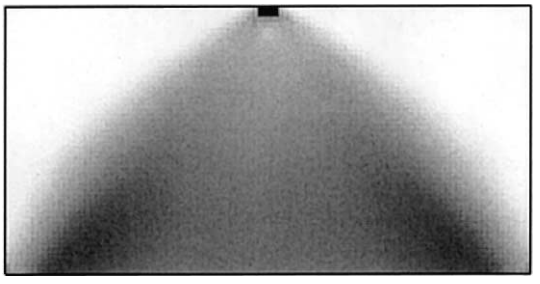

Fig. 6. Composite solution for the cantilever 2×1.

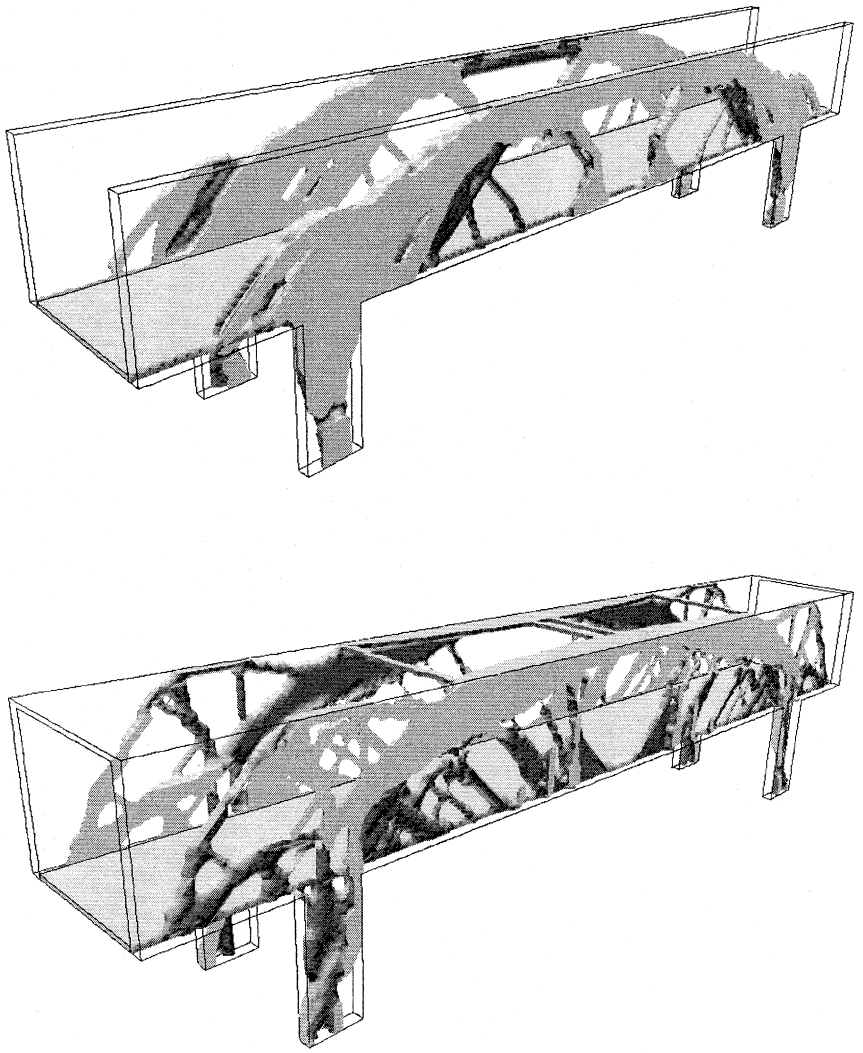

Fig. 7. Two optimal bridges for different workspaces.

As a last numerical example, we show in Fig. 7, two tridimensional computations of a bridge. The roadway is not submitted to optimization. Its density is 3 while the density of the material used for optimization is 1. The Lamé coefficients are the same for both subdomains. The first eigenvalue has been optimized and the quite different designs have been obtained by changing the workspace (solid lines on the pictures). In the second case, horizontal links at the top of the structure are allowed. A volume constraint of 30% of the total volume has been imposed in both cases. The penalized solution is drawn, showing the contour plot of the density θ for $\theta > 0.4$.

References

[1] G. Allaire, Z. Belhachmi, F. Jouve, The homogenization method for topology and shape optimization. Single and multiple loads case, Revue Européenne des Eléments Finis 5 (1996) 649–672.
[2] G. Allaire, E. Bonnetier, G. Francfort, F. Jouve, Shape optimization by the homogenization method, Nümerische Mathematik 76 (1997) 27–68.
[3] G. Allaire, R.V. Kohn, Optimal bounds on the effective behavior of a mixture of two well-ordered elastic materials, Quat. Appl. Math. 51 (1993) 643–674.

[4] G. Allaire, R.V. Kohn, Optimal design for minimum weight and compliance in plane stress using extremal microstructures, Eur. J. Mech. A/Solids 12 (6) (1993) 839–878.
[5] M. Avellaneda, Optimal bounds and microgeometries for elastic two-phase composites, SIAM J. Appl. Math. 47 (6) (1987) 1216–1228.
[6] M. Bendsoe, Methods for Optimization of Structural Topology, Shape and Material, Springer, Berlin, 1995.
[7] M. Bendsoe, A. Diaz, Optimization of material properties for improved frequency response, Struct. Optim. 7 (1994) 138–140.
[8] M. Bendsoe, N. Kikuchi, Generating optimal topologies in structural design using a homogenization method, Comput. Methods Appl. Mech. Engrg. 71 (1988) 197–224.
[9] M. Bendsoe, C. Mota Soares (Eds.), Topology Optimization of Structures, Nato ASI Series E, Kluwer Academic Publishers, Dordrecht, 1993.
[10] A. Cherkaev, R. Palais, Optimal design of three-dimensional axisymmetric elastic structures, in: N. Olhoff, G. Rozvany (Eds.), Proceedings of the First World Congress of Structural and Multidisciplinary Optimization, Pergamon Press, Oxford, 1995, pp. 201–206.
[11] S. Cox, R. Lipton, Extremal eigenvalue problems for two-phase conductors, Arch. Rat. Mech. Anal. 136 (1996) 101–117.
[12] G. Dal Maso, R. Kohn, The local character of G-closure, unpublished work.
[13] A. Diaz, N. Kikuchi, Solutions to shape and topology eigenvalue optimization problems using a homogenization method, Int. J. Numer. Methods Engrg. 35 (1992) 1487–1502.
[14] J. Folgado, H. Rodrigues, Structural optimization with a non-smooth buckling load criterion, Control and Cybernetics 27 (1998) 235–253.
[15] G. Francfort, F. Murat, Homogenization and optimal bounds in linear elasticity, Arch. Rat. Mech. Anal. 94 (1986) 307–334.
[16] L. Gibianski, A. Cherkaev, Design of composite plates of extremal rigidity, Preprint, Ioffe Physicotechnical Institute, 1984. (English translation in: Topics in the mathematical modeling of composite materials, in: A. Cherkaev, R.V. Kohn (Eds.), Progress in Nonlinear Differential Equations and their Applications, Birkhaüser, Boston, 1997).
[17] V. Jikov, S. Kozlov, O. Oleinik, Homogenization of Differential Operators, Springer, Berlin, 1995.
[18] C. Jog, R. Haber, M. Bendsoe, Topology design with optimized, self-adaptative materials, Int. J. Numer. Methods Engrg. 37 (1994) 1323–1350.
[19] T. Kato, Perturbation Theory for Linear Operators, Springer, Berlin, 1966.
[20] R. Kohn, G. Strang, Optimal design and relaxation of variational problems I, Commun. Pure Appl. Math. 39 (1986) 113–137.
[21] R. Kohn, G. Strang, Optimal design and relaxation of variational problems II, Commun. Pure Appl. Math. 39 (1986) 139–182.
[22] R. Kohn, G. Strang, Optimal design and relaxation of variational problems III, Commun. Pure Appl. Math. 39 (1986) 353–377.
[23] R. Kohn, R. Lipton, Optimal bounds for the effective energy of a mixture of isotropic, incompressible, elastic materials, Arch. Rat. Mech. Anal. 102 (4) (1988) 331–350.
[24] L. Krog, N. Olhoff, Topology optimization of plate and shell structures with multiple eigenfrequencies, in: N. Olhoff, G. Rozvany (Eds.), Proceedings of the First World Congress of Structural and Multidisciplinary Optimization, Pergamon Press, Oxford, 1995, pp. 675–682.
[25] R. Lipton, A saddle-point theorem with application to structural optimization, J. Optim. Th. Appl. 81 (3) (1994) 549–567.
[26] K. Lurie, A. Cherkaev, A. Fedorov, Regularization of optimal design problems for bars and plates I, J. Optim. Th. Appl. 37 (1982) 499–521.
[27] K. Lurie, A. Cherkaev, A. Fedorov, Regularization of optimal design problems for bars and plates II, J. Optim. Th. Appl. 37 (1982) 523–543.
[28] Z. Ma, N. Kikuchi, H. Cheng, I. Hagiwara, Topology and shape optimization methods for structural dynamic problems, in: P. Pedersen (Ed.), Optimal Design with Advanced Materials, Elsevier, Amsterdam, 1993, pp. 247–261.
[29] F. Murat, Contre-exemples pour divers problèmes où le contrôle intervient dans les coefficients, Ann. Mat. Pura Appl. 112 (1977) 49–68.
[30] F. Murat, L. Tartar, *H*-convergence, in: Topics in the mathematical modeling of composite materials, in: A. Cherkaev, R.V. Kohn (Eds.), Progress in Nonlinear Differential Equations and their Applications, Birkhaüser, Boston, 1997. French version: mimeographed notes, séminaire d'Analyse Fonctionnelle et Numérique de l'Université d'Alger, 1978.
[31] F. Murat, L. Tartar, Calcul des Variations et Homogénéisation, Les Méthodes de l'Homogénéisation Théorie et Applications en Physique, Coll. Dir. Etudes et Recherches EDF, Eyrolles (1985) 319–369. (English translation in: Topics in the mathematical modeling of composite materials, in: A. Cherkaev, R.V. Kohn (Eds.), Progress in Nonlinear Differential Equations and their Applications, Birkhaüser, Boston, 1997).
[32] M.M. Neves, H. Rodrigues, J.M. Guedes, Generalized topology design of structures with a buckling load criterion, Struct. Optim. 10 (1995) 71–78.
[33] O. Oleinik, A. Shamaev, G. Yosifian, On the convergence of the energy, stress tensors and eigenvalues in homogenization problems of elasticity, Z. Angew. Math. Mech. 65 (1985) 13–17 1985.
[34] J. Sanchez-Hubert, E. Sanchez-Palencia, Vibration and Coupling of Continuous systems. Asymptotic Methods, Springer, Berlin, 1989.
[35] O. Sigmund, Design of material structures using topology optimization, Ph.D. Thesis, Report S 69, Department of Solid Mechanics, Technical University of Denmark, 1994.
[36] K. Suzuki, N. Kikuchi, A homogenization method for shape and topology optimization, Comput. Methods Appl. Mech. Engrg. 93 (1991) 291–318.
[37] M. Zhou, G. Rozvany, The COC algorithm, Part II: Topological, geometrical and generalized shape optimization, Comput. Methods Appl. Mech. Engrg. 89 (1991) 309–336.